# Carbon Nanotubes and Spheres Produced by Modified Ferrocene Pyrolysis

Haoqing Hou,* Andreas K. Schaper, Frank Weller, and Andreas Greiner

*Department of Chemistry & Materials Science Center, Philipps-University of Marburg, D-35032 Marburg, Germany*

*Received May 21, 2002. Revised Manuscript Received June 27, 2002*

Single-wall carbon nanotubes (SWCNTs) and well-aligned thin multiwall carbon nanotubes (MWCNTs) were successfully synthesized via pyrolysis of a powder mixture of ferrocene and anthracene or 9,10-dibromoanthracene. It is shown that the size of the MWCNTs can be tuned just by changing the ratio of ferrocene/anthracene in the mixture. A lower ratio resulted in low-diameter MWCNTs containing up to five graphene layers only; a high ratio has led to thick MWCNTs with more than 25 layers. Furthermore, there are two extreme cases, the pyrolysis of powders at a low ratio of 1:7 that gives rise to carbon nanospheres and the pyrolysis of pure ferrocene in a $H_2$ flow that mainly gives rise to metal nanoparticles. When powder mixtures of ferrocene and 9,10-dibromoanthracene are pyrolyzed, both SWCNTs and spherical carbon-coated iron nanoparticles are obtained.

## 1. Introduction

Since their first observation in 1991,[1] carbon nanotubes (CNTs) have been one of the most actively studied materials because of their unique structure and extraordinary mechanical[2,3] and electronic[4−6] properties. Synthesis methods for single-wall (SWCNTs) and multiwall carbon nanotubes (MWCNTs) include arc-discharge,[1,7] laser ablation,[8] gas-phase catalytic growth from carbon monoxide,[9] chemical vapor deposition (CVD) from hydrocarbons,[10−13] and various template methods.[14,15] A step toward commercial realization are the large-scale production routes realized by pyrolysis of organometallic compounds, such as iron(II) phthalocyanine,[16,17] nickel phthalocyanine,[18] and ferrocene,[19,20] in particular.

In catalytic growth, the amount of carbon delivered from the precursor plays a decisive role in the CNT formation process.[21,22] In a metallocene molecule the metal-to-carbon ratio is 1/10 or less so that the total amount of carbon input will be insufficient to yield pure SWCNTs or MWCNTs. Furthermore, the particular shape and structure of the CNTs, their diameter and the wall thickness, appear to be strongly determined by the amount and the size of metal particles remaining after decomposition of the metallocene.[17,23] Even these parameters depend on the balance of the decomposition reaction. Synthesis and tailoring of different formations of carbon nanotubes makes necessary, therefore, the use of additional carbon sources. Various hydrocarbons, such as *p*-xylene,[20,24−27] acetylene,[19] benzene,[21,22] and

* To whom correspondence should be addressed: Department of Chemistry, Institute of Physical, Nuclear and Macromolecular Chemistry, Philipps-University Marburg, Hans-Meerwein-Str., D-35032 Marburg, Germany. Phone: +49 6421 282-5573. Fax: +49 6421 282-5785. E-mail: haoqing@chemie.uni-marburg.de.

(1) Iijma, S. *Nature* **1991**, *354*, 56.
(2) Treacy, M. M. J.; Ebbesen, T. W.; Gibson, J. M. *Nature* **1996**, *381*, 678.
(3) Walters, D. A.; Ericson, L. M.; Casavant, M. J.; Liu, J.; Colbert, D. T.; Smith, K. A.; Smalley, R. E. *Appl. Phys. Lett.* **1999**, *74*, 3803.
(4) de Heer, W. A.; Chatelain, A.; Ugarte, D. *Science* **1995**, *270*, 1179.
(5) Zhu, W.; Bower, C.; Zhou, O.; Kochanski, G.; Jin, S. *Appl. Phys. Lett.* **1999**, *75*, 873.
(6) Fan, S.; Chapline, M. G.; Franklin, N. M.; Tombler, T. W.; Cassell, A. M.; Dai, H. *Science* **1999**, *283*, 512.
(7) Journet, C.; Maser, W. K.; Bernier, P.; Loiseau, A.; de la Chapelle, M. L.; Lefrant, S.; Lee, R.; Fischer, J. E. *Nature* **1997**, *388*, 756.
(8) Rinzler, A. G.; Liu, J.; Dai, H.; Nikolaev, P.; Huffman, C. B.; Rodriguez-Macias, F. J.; Boul, P. J.; Lu, A. H.; Heyman, D.; Colbert, D. T.; Lee, R. S.; Fischer, J. E.; Rao, A. M.; Eklund, P. C.; Smalley, R. E. *Appl. Phys. A* **1998**, *67*, 29.
(9) Nikolaev, P.; Bronikowski, M. J.; Bradley, R. K.; Fohmund, F.; Colbert, D. T.; Smith, K. A.; Smalley, R. E. *Chem. Phys. Lett.* **1999**, *313*, 91.
(10) Ren, Z. F.; Huang, Z. P.; Wang, D. Z.; Wen, J. G.; Xu, J. W.; Wang, J. H.; Calvet, L. E.; Chen, J.; Klemic, J. F.; Reed, M. A. *Appl. Phys. Lett.* **1999**, *75*, 1086.
(11) Ren, Z. F.; Huang, Z. P.; Xu, J. W.; Wang, J. H.; Bush, P.; Siegal, M. P.; Provencio, P. N. *Science* **1998**, *282*, 1105.
(12) Huang, Z. P.; Xu, J. W.; Ren, Z. F.; Wang, H. J.; Siegal, M. P.; Provencio, P. N. *Appl. Phys. Lett.* **1998**, *73*, 3845.
(13) Tang, Y. H.; Zheng, Y. F.; Lee, C. S.; Wang, N.; Lee, S. T.; Sham, T. K. *Chem. Phys. Lett.* **2001**, *342*, 259.
(14) Che, G.; Lakshmi, B. B.; Martin, C. R.; Fisher, E. R.; Ruoff, R. S. *Chem. Mater.* **1998**, *10*, 260.
(15) Wang, N.; Tang, Z. K.; Li, G. D.; Chen, J. S. *Nature* **2000**, *408*, 50.
(16) Huang, S.; Dai, L.; Mau, A. W. H. *J. Phys. Chem. B* **1999**, *103*, 4223.
(17) Li, D. C.; Dai, L.; Huang, S.; Mau, A. W. H.; Wang, Z. L. *Chem. Phys. Lett.* **2000**, *316*, 349.
(18) Yudasaka, M.; Kikuchi, R.; Ohki, Y.; Yoshimura, S. *Carbon* **1997**, *35*, 195.
(19) Rao, C. N. R.; Sen, R.; Satishkumar, B. C.; Govindaraj, A. *Chem. Commun.* **1998**, *15*, 1525.
(20) Andrews, R.; Jacques, D.; Rao, A. M.; Derbyshire, F.; Qian, D.; Fan, X.; Dickey, E. C.; Chen, J. *Chem. Phys. Lett.* **1999**, *303*, 467.
(21) Cheng, H. M.; Li, F.; Su, G.; Pan, H. Y.; He, L. L.; Sun, X.; Dresselhaus, M. S. *Appl. Phys. Lett.* **1998**, *72*, 3282.
(22) Sen, R.; Govindaraj, A.; Rao, C. N. R. *Chem. Phys. Lett.* **1997**, *267*, 276.
(23) Choi, Y. C.; Shin, Y. M.; Lee, Y. H.; Lee, B. S.; Park, G. S.; Choi, W. B.; Lee, N. S.; Kim, J. M. *Appl. Phys. Lett.* **2000**, *76*, 2367.
(24) Cao, A.; Ci, L.; Li, D.; Wei, B.; Xu, J.; Liang, J.; Wu, D. *Chem. Phys. Lett.* **2001**, *335*, 150.
(25) Cao, A.; Zhu, H.; Zhang, X.; Li, X.; Ruan, D.; Xu, C.; Wei, B.; Liang, J.; Wu, D. *Chem. Phys. Lett.* **2001**, *342*, 510.

10.1021/cm021206x CCC: $22.00 
Published on Web 08/15/2002

**Table 1. Synthesis Conditions and Properties of Nanoparticles Prepared by Modified, Ferrocene-Based Pyrolysis**

| sample | gas flow (300−400 mL/min) | pyrolysis temperature (°C) | F/A[a] | contents (g) | yield (mg) | trait of product | outer diameter (nm) |
|---|---|---|---|---|---|---|---|
| A | $H_2$ | 580−700 | 1/1 | 1 | 452 | aligned MWNTs | 30−60 (>25)[b] |
| B | $H_2$ | 580−700 | 1/2 | 1 | 294 | aligned MWNTs | 10−30 (<15)[b] |
| C | $H_2$ | 580−700 | 1/2.5 | 1 | 205 | aligned MWNTs | 5−25 (<10)[b] |
| D | $H_2$ | 580−700 | 1/7 | 1 | 63 | nanospheres | 100−200 |
| E | $H_2$ | 580−700 | 1/0 | 1 | 761 | nanospheres | 50−150 |
| F | Ar | 900−1000 | 1/0 | 1 | 658 | nanospheres | 100−200 |
| G | Ar | 1000−1100 | 1/1[c] | 0.5 | 50−110 | SWNTs + MWNTs | 0.8−1.5 + 20−50 |

[a] F = ferrocene; A = anthracene. [b] Number of graphene layers. [c] 9,10-Dibromoanthracene.

others, have proved to be suitable carbon dispensers in mixtures with a metallocene.

Recently, increasing work has been focused on growth methods leading to well-aligned CNTs over large areas to form nanotube arrays. With use of CVD, large CNT arrays were successfully grown on different substrates such as mesoporous silica,[28,29] quartz glass,[11,20,24] Au film,[24] and existing CNT arrays,[26] under the catalytical activity of Fe, Ni, or Co. The alignment of nanotubes is highly desired for potential applications in vacuum microelectronics and flat panel displays.[11,30,31] CNTs filled with ferromagnetic material are of particular interest for the development of data storage systems, toners, and inks for xerography.[32]

In this paper we report on the synthesis of aligned carbon nanotubes by the pyrolysis of mixtures of ferrocene with anthracene and anthracene derivatives as new additional carbon precursors. The pyrolysis parameters that control the variation of the wall thickness of the nanotubes between single walls and multiwalls are systematically studied.

## 2. Experimental Section

**Materials.** Hydrogen (Messer), ferrocene (98%, Acros), anthracene (98%, Aldrich), and 9,10-dibromoanthracene (99%, Aldrich) were used as received. A silicon wafer (both sides polished, Wacker Siltronic) was cut into 3 × 6 cm slide pieces and washed with acetone two times before use.

**Synthesis Apparatus.** The experimental setup, depicted schematically in Figure 1, is almost identical to the equipment reported previously.[33] The pyrolysis reactor (inner diameter of the quartz glass tube 35 mm, effective heating length 650 mm) is heated by a dual furnace fitted with independent temperature controllers. Two different vaporization zones A and B have been used; the pyrolysis products were deposited on a Si wafer substrate or on quartz glass at position C or on a glass surface at room temperature at position D.

**CNT Synthesis.** One gram of powder mixture of ferrocene and anthracene (1:1 mole ratio) was placed into the vaporization chamber. The mixture was vaporized at 160−200 °C and carried by the hydrogen flow (300−400 mL/min) into the quartz tube, where the pyrolysis was performed in a $H_2$ atmosphere at 580−700 °C. The resulting MWCNTs grew both on the silicon substrate and on the wall of the quartz tube as a black mat-like layer that could be scraped off. SWCNTs were synthesized by placing 0.5 g of a 1:1 fine powder mixture of ferrocene and 9,10-dibromoanthracene into part I of the reactor tube and then heating this part gradually up to 400 °C. The temperature in part II was 1000−1100 °C; the reaction was accomplished under a 400 mL/min Ar flow atmosphere. The sample run, the composition ratio of the starting material, and the reaction yield of the pyrolysis experiment are listed in Table 1.

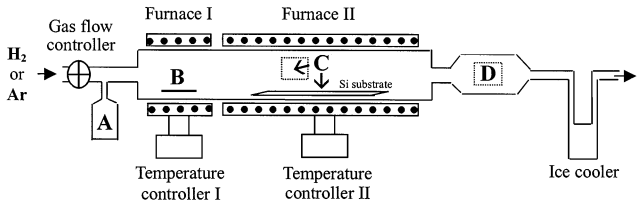


**Figure 1.** Schematic diagram of the apparatus used for the synthesis of CNTs. (A and B) vaporization sources; (C) deposition on Si or quartz glass substrate; (D) room-temperature deposition on a normal glass surface.

**Measurements.** Characterization of the CNTs was performed by scanning electron microscopy (SEM) using CamScan 4 at 15-kV accelerating voltage, equipped with a NORAN energy-dispersive X-ray (EDX) detector, as well as by transmission electron microscopy (TEM) using a JEM 3010 operated at 300 kV. Raman spectroscopic measurements were carried out using a Jobin-Yvon LABRAM HR800 Ar laser with 514.5-nm excitation. Wide-angle X-ray scattering (WAXS) investigations were performed using a Siemens D5000 and Cu Kα radiation.

## 3. Results

**3.1. Nanospheres.** Without any additional carbon source, the pyrolysis of pure ferrocene at 580−700 °C resulted in almost spherical Fe nanoparticles with diameters on the order of 10 nm, which were surrounded by some carbon material (Figure 2a. No CNTs were observed under these conditions. However, when the pyrolysis temperature was increased to 900−1000 °C, a limited amount of nanotube material was found among the dominating spherical particles and particle aggregations (Figure 2b).

**3.2. Aligned Multiwall Nanotubes.** When anthracene is used as a new additional carbon source, the pyrolysis of the mixture of ferrocene and anthracene at 580−700 °C leads to densely packed carbon nanotubes aligned perpendicular to the substrate as shown in Figure 3a. The nanotube array exhibits a homogeneous thickness, that is, constant tube length, of about 10 μm. The tubes are straight and well-aligned if not deformed

(26) Sun, L. F.; Liu, Z. Q.; Ma, X. C.; Zhong, Z. Y.; Tang, S. B.; Xiong, Z. T.; Tang, D. S.; Zhou, W. Y.; Zou, X. P.; Li, Y. B.; Tan, K. L.; Xie, S. S.; Lin, J. Y. *Chem. Phys. Lett.* **2001**, *340*, 222.
(27) Cao, A.; Xu, C.; Liang, J.; Wu, D.; Wei, B. *Chem. Phys. Lett.* **2001**, *344*, 13.
(28) Li, W. Z.; Xie, S. S.; Qian, L. X.; Chang, B. H.; Zou, B. S.; Zhou, W. Y.; Zhao, R. A.; Wang, G. *Science* **1996**, *274*, 1701.
(29) Li, W.; Zhang, H.; Wang, C.; Zhang, Y.; Xu, L.; Zhu, K.; Xie, S. *Appl. Phys. Lett.* **1997**, *70*, 2684.
(30) Ajayan, P. M.; Ebbesen, T. W. *Rep. Prog. Phys.* **1997**, *60*, 1026.
(31) Saito, R.; Dresselhaus, G.; Dresselhaus, M. S. *Physical Properties of Carbon Nanotubes*; Imperial College Press: London, 1998.
(32) Murakami, H.; Hirakawa, M.; Tanaka, C.; Yamakawa, H. *Appl. Phys. Lett.* **2000**, *76*, 1776.
(33) Schaefer, O.; Greiner, A.; Pommerehne, J.; Guss, W.; Vestweber, H.; Tak, H. Y.; Baessler, C.; Schmidt, C.; Luessem, G.; Shartel, B.; Stuempflen, V.; Wendorff, J. H.; Spiegel, S.; Moeller, C.; Spiess, H. W. *Synth. Met.* **1996**, *82*, 1.

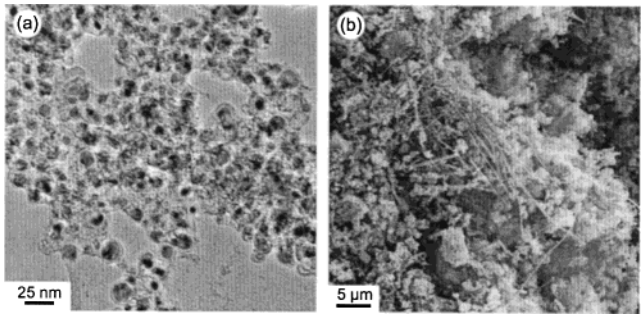


**Figure 2.** Pyrolysis of pure ferrocene (a) at 580−700 °C, leading to carbon-coated Fe particles (TEM) and (b) at 900−1000 °C, leading to Fe particles along with a small number of CNTs (SEM).

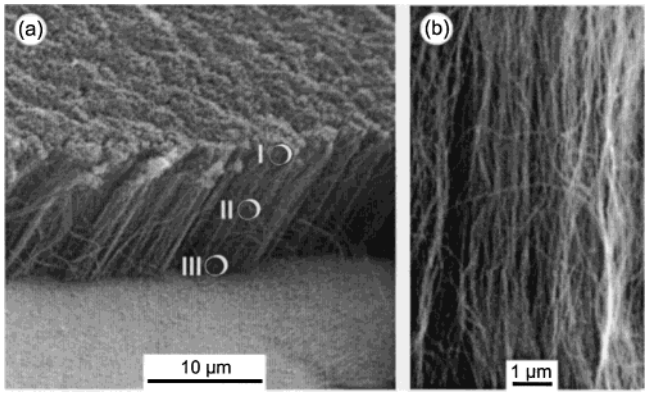


**Figure 3.** Scanning electron micrographs of an extended array of well-aligned CNTs with areas of EDX analysis indicated (a); peeled-off part of the array at higher magnification (b).

by the peeling preparation as in the higher magnification micrograph in Figure 3b.

Viewing the array mats edge-on, we have performed EDX elemental analysis of selected areas of tube ensembles across the mat thickness as indicated in Figure 3a. Under the same conditions, an average Fe content of 15 wt % was determined for the top surface (position I), 2.5 wt % in the middle part (position II) and 5 wt % at the bottom (position III) of sample B as grown on a silicon substrate. The nominal overall Fe content of this sample was 6.78 wt %. As a typical result, the catalyst particles are mainly present at the top surface of an array and, to some extent, in the bottom. The middle part is usually almost free of metal.

We have studied the fine structure of the CNTs from such arrays using high-resolution transmission electron microsopy (HRTEM). The electron micrographs in Figure 4 demonstrate systematic changes of the tube structure with varying ferrocene/anthracene (F/A) ratio at otherwise same pyrolysis conditions. Already in the medium magnification images of parts a−c of Figure 4, the differences between the CNTs from samples A (F/A = 1.0), B (F/A = 0.5), and C (F/A = 0.4) are striking. The outer diameter of the CNTs decreases from about 45 nm (a) to 15 nm (c) with increasing anthracene content. At some places, an iron catalyst particle can be detected at the end of a nanotube. At higher resolution, parts d−f of Figure 4 enable us to determine the wall thickness by counting the number of graphene layers. On the average, in sample A one measures 25 layers, in sample B 10 layers, and in sample C 5 layers. The lattice plane ordering is not perfect; with decreasing

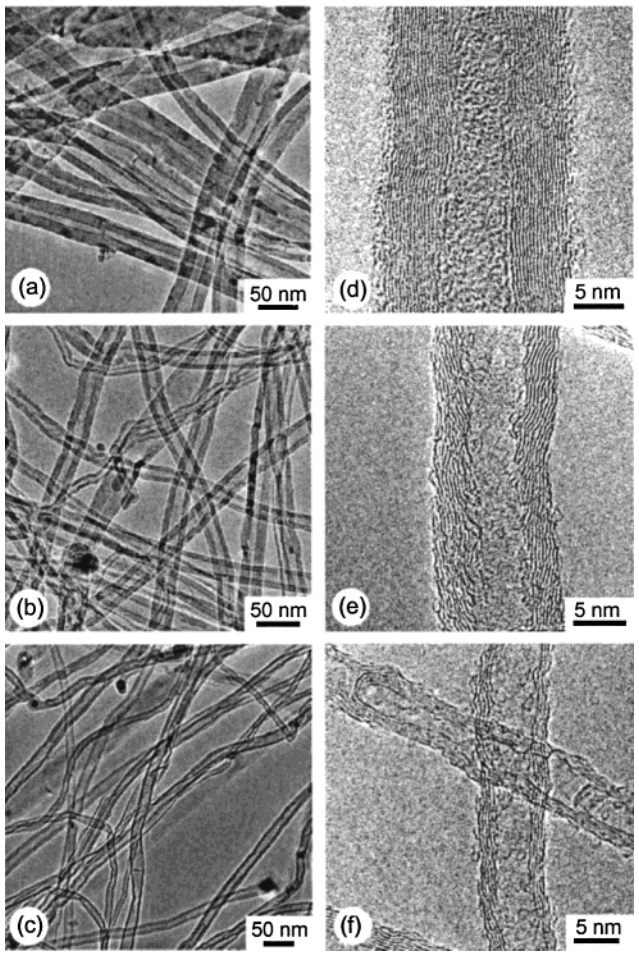


**Figure 4.** Transmission electron micrographs of MWCNTs synthesized from ferrocene/anthracene mixtures at the ratio 1:1 (a,d), 1:2 (b, e), and 1:2.5 (c,f). From the high-resolution images (d−f) a continuous decrease in diameter and wall thickness can be deduced.

diameter the walls become increasingly staggered with more layers crossing the lumen of the tubes.

Raman characterization of the products A, B, and C revealed the typical features of MWCNTs without any significant difference between the samples (not shown here). The peak frequencies exhibited the graphite mode at 1579 $cm^{-1}$ and contain disorder modes at 1351, 1617, 2698, and 3226 $cm^{-1}$ and the combination of a graphitic and disorder line at 2946 $cm^{-1}$.[31,34,35]

Finally, any further reduction of the ferrocene/anthracene ratio (sample D) changes the structure formation process toward the growth of large quantities of spherical carbon nanoparticles (Figure 5), rather tube-like particles.

**3.3. Single-Wall Nanotubes.** Variation of the pyrolysis conditions using 9,10-dibromoanthracene as a new carbon precursor in a 1:1 mixture with ferrocene at 1000−1100 °C and depositing the synthesis product at room temperature in part D of the apparatus resulted in the formation of SWCNTs and bundles of SWCNTs between finely dispersed Fe nanospheres in sample G. SEM and TEM images of SWCNTs are shown in parts

(34) Ravindran, T. R.; Jackson, B. R.; Badding, J. V. *Chem. Mater.* **2001**, *13*, 4187.
(35) Li, W.; Zhang, H.; Wang, C.; Zhang, Y.; Xu, L.; Zhu, K.; Xie, S. *Appl. Phys. Lett.* **1997**, *70*, 2684.

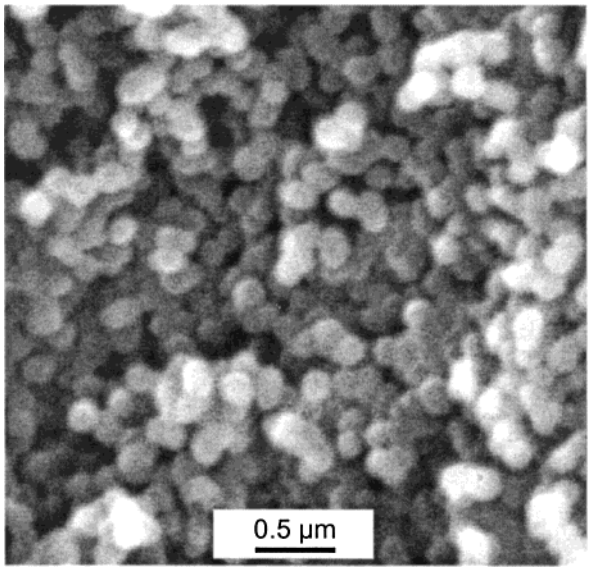


**Figure 5.** SEM of carbon nanospheres obtained by pyrolysis of a 1:7 mixture of ferrocene and anthracene.

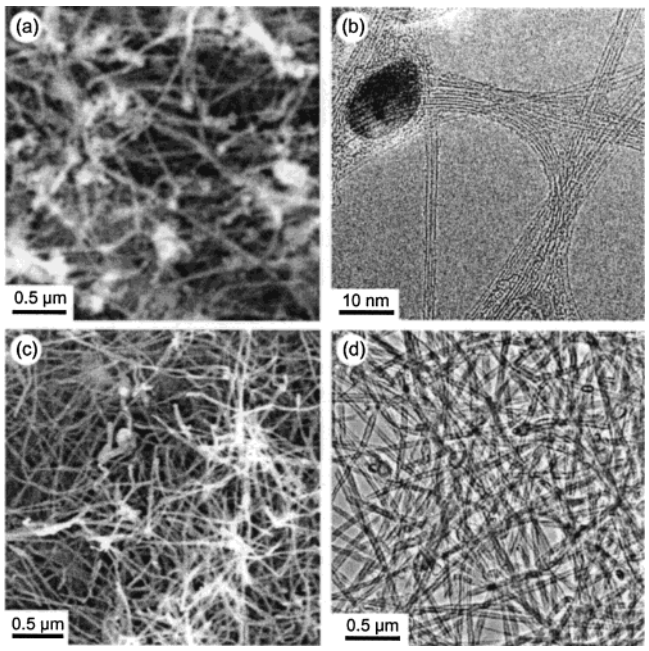


**Figure 6.** SEM and TEM micrographs of SWCNTs obtained by pyrolysis of a ferrocene/9,10-dibromoanthracene precursor and deposited (a,b) on a glass surface at place D in Figure 1 and (c,d) on a silicon substrate, position C in Figure 1.

a and b of Figure 6. In parallel with these SWCNTs depositions, large amounts of nonaligned thin multiwall CNTs are formed by deposition on silicon and on quartz glass substrate at elevated temperature in part C of the reactor. Examples are displayed in Figure 6c,d.

The Raman spectrum of the SWCNT-containing pyrolysis product shows several obvious radial breathing mode (RBM) peaks clearly featuring SWCNTs (Figure 7). The corresponding diameters of the SWCNTs were calculated to be 1.21, 1.08, 1.02, 0.90, 0.85, 0.82, and 0.77 nm using the approach reported by Rao et al.[36] Those estimations agree well with the TEM observations made in Figure 4.

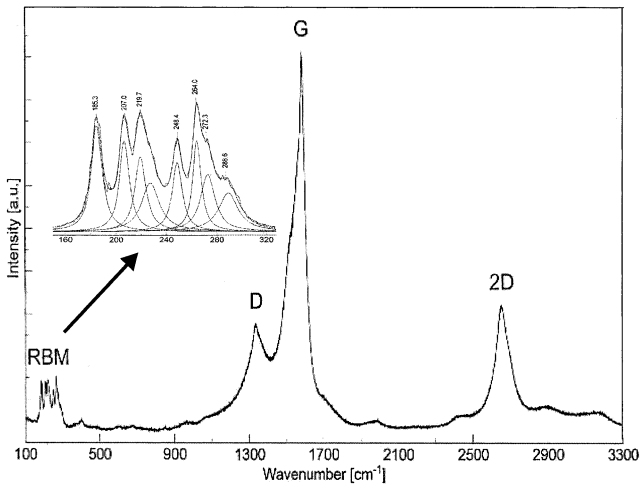


**Figure 7.** Typical Raman spectrum of sample G displaying clear RBM peaks featuring SWCNTs.

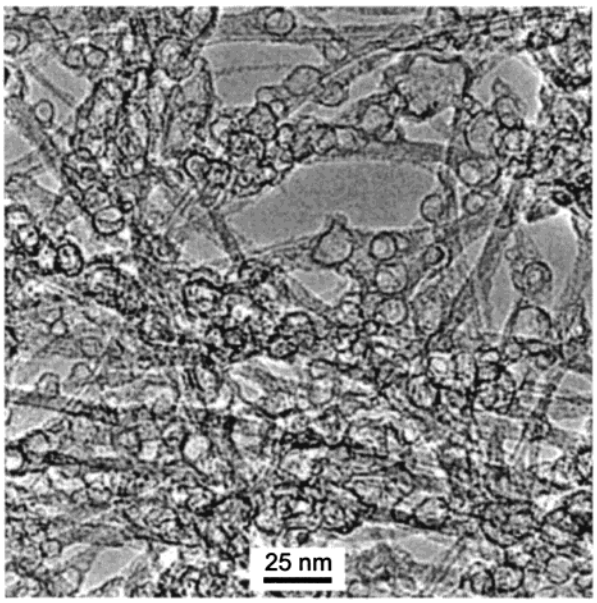


**Figure 8.** TEM micrograph of sample G after annealing at 1000−1100 °C in an Ar atmosphere for 4 h, showing SWCNTs together with hollow carbon spheres with the encapsulated iron particles removed.

Annealing of sample G at 1000−1100 °C under an Ar flow of 300−400 mL/min completely removed the iron from the orignally iron-bearing nanoparticles, resulting in hollow carbon nanospheres along with pure SWCNTs (Figure 8).

## 4. Discussion

Ferrocene is a highly volatile organometallic compound with excellent vaporizability. Its decomposition temperature in the gas phase was reported to be higher than 400 °C.[37] In our experiments, decomposition of ferrocene in the gas phase at 580−700 and 900−1000 °C yielded spherical carbon-coated Fe particles. The impossibility to get CNTs in this process is due to the low carbon/iron ratio in pure ferrocene. This result is confirmed by the reported formation of iron nanorods with carbon-coating layers when the pyrolysis of fer-

(36) Rao, A. M.; Bandow, S.; Richter, E.; Eklund, P. C. *Thin Solid Films* **1998**, *331*, 141.

(37) Bernhauer, M.; Braun, M.; Huettinger, K. J. *Carbon* **1994**, *32*, 1073.

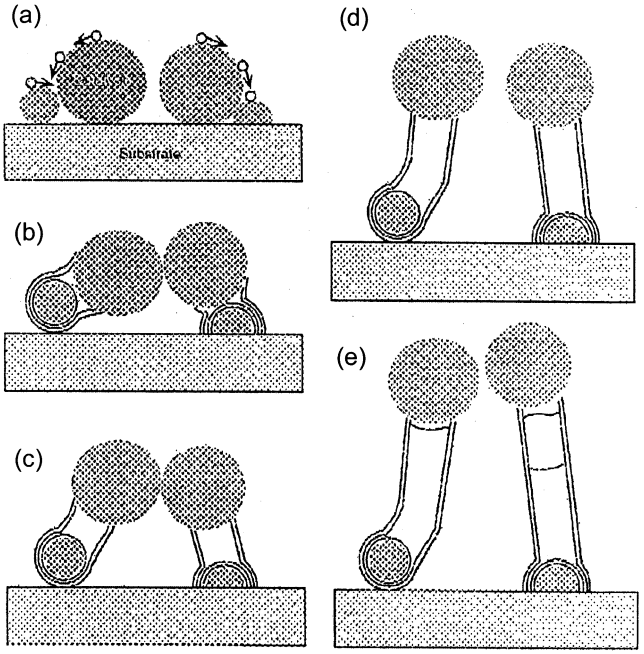


**Figure 9.** Schematic of the growth mechanism of aligned MWCNTs on a flat substrate (reproduced with permission from ref 17). Carbon atoms deposited on the surface of iron particles are of high mobility (a) and form graphitic shells in the neck region between differently sized particles (b). During extension of the graphene sheets the head-on contact between adjacent iron particles forces the nanotubes to grow vertically (c). Thereby, the incorporation of defects into the hexagonal carbon network results in curling of the tubes (d) and in the formation of carbon bridges, yielding a bamboo-like structure (e).

rocene is performed between 1170 and 1370 °C under vacuum or Ar flow.[19]

In the present paper we have introduced anthracene as a promising additional carbon source for the production of CNTs by the metallocene catalyst route. The mixture of ferrocene and anthracene is vaporized and directed into the high-temperature furnace region, where it is decomposed to form small Fe and $C_n$ clusters. Iron is an effective catalyst of hydrogenation and dehydrogenation reactions; its catalyzing capability, for example, in the pyrolysis of pitch, has been known for a long period of time.[37] The pyrolysis of the ferrocene/anthracene mixture of different composition ratios at temperatures between 580 and 700 °C results in well-aligned MWCNTs in the diameter range 5−50 nm, forming nanotube arrays both on a silicon substrate and on quartz glass. The initiation by the nanoparticulate Fe surface and the mechanism of aligned carbon nanotube growth can be understood on the basis of the considerations of Li et al.[17] illustrated in Figure 9. Our observations confirm the findings of other authors[17,38] that the remaining catalyst particles are favorably concentrated within the top layer of the tube array, which is a clear illustration of the proposed growth mechanism.

From Figure 4 we have seen that the diameter and the wall thickness of the CNTs decreased with the increase of the anthracene content in the mixture. According to the model in Figure 9, it is reasonable to suppose that the large diameter CNTs will originate from the catalytic iron nanoparticles with large size and the small diameter CNTs from the small catalytic species. The size of the nanoparticles is obviously controlled by the amount of additional carbon precursor in the mixture with ferrocene. At low percentage of iron in the high-temperature reacting vapor, the tendency of the atoms to aggregate is reduced; thus, only small-sized iron nanoparticles will be formed and vice versa. As it becomes clear from the growth model in Figure 9, the small diameter CNTs generally show a thinner tube wall containing only a few graphitic layers as compared to the large diameter CNTs. However, further reduction of the amount of ferrocene in the mixture (sample D) does not lead to progressive thinning of the CNTs and is, thus, not a suitable route toward SWCNTs. Instead, large amounts of carbon nanospheres are formed via carbonization of anthracene at high temperature.

However, while the pyrolysis of a low ratio ferrocene/anthracene powder mixture does not result in the formation of SWCNTs, the pyrolysis of ferrocene with 9,10-dibromoanthracene under an Ar atmosphere does. The reason for this different reaction behavior of the two precursor materials has remained unclear to the present time. On the other hand, the fact that the Fe in the additionally formed encapsulated iron particles already melts at temperatures as low as 1000−1100 °C under Ar flow points to the changed behavior of nano-sized particles as compared to the bulk where the melting point is 1535 °C. In other experiments we have observed in situ the diffusion of Cu through the shells of carbon nanospheres under vacuum during annealing at elevated temperature. These findings will be reported elsewhere.[39]

## Conclusions

With introduction of the new additional carbon precursor anthracene, large-scale well-aligned thin MWCNT arrays were synthesized by pyrolysis of powder mixtures of ferrocene and the precursor at temperatures of 580−700 °C under $H_2$ flow. The diameter and the wall thickness of the nanotubes can be tuned by changing the amount of ferrocene in the mixture. SWCNTs are obtained in the pyrolysis of mixtures of ferrocene with 9,10-dibromoanthracene at 1000−1100 °C under an Ar flow. In both cases, the pyrolysis of pure ferrocene and of ferrocene/dibromoanthracene mixtures under $H_2$ flow, besides the CNTs, iron nanoparticles with carbon covering are formed, from which hollow nanospheres can be obtained when the Fe is removed by annealing at elevated temperature.

CM021206X

(38) Thien-Nga, L.; Hernadi, K.; Forro, L. *Adv. Mater.* **20001**, *13*, 148.

(39) Schaper, A. K.; Hou, H.; Greiner, A.; Phillipp, F., in preparation.